

# Ocular migration and the metamorphic and postmetamorphic maturation of the retinotectal system in *Xenopus laevis*: an autoradiographic and morphometric study

S. GRANT\* AND M. J. KEATING

*Division of Neurophysiology and Neuropharmacology, National Institute for Medical Research, Mill Hill, London, NW7 1AA, UK*

---

## SUMMARY

The growth of the retina and tectum during larval life in *Xenopus* has previously been studied extensively. These two structures continue to grow in metamorphosing and postmetamorphic animals. During these later stages there are marked changes in eye position. We have used histogenetic and morphometric techniques to monitor retinal and tectal growth in *Xenopus* aged from stage 58 of larval life to ten years postmetamorphosis. The relative eye migration was quantified with optical techniques. An attempt has been made to relate modes of retinal growth to problems associated with changing interocular geometry.

The predominant mode of growth during this period is hypertrophic, that is, it is due largely to an increase in size and complexity of existing elements, rather than the histogenetic creation of new elements. In the retina, however, tritiated thymidine autoradiography reveals that histogenesis does persist until at least six months after metamorphosis. The rate of histogenesis is much decreased compared with that of larval stages but, like that of larval stages, it takes place at the ciliary margin. It is asymmetrically distributed in the retina, most histogenesis occurring at the ventral retinal pole and very little at the dorsal retinal pole. Some histogenesis occurs at the nasal and temporal retinal poles. Thymidine autoradiography and cell counts indicated that little significant histogenesis occurs in the tectum after metamorphic climax.

Two possible biological reasons for the asymmetry of retinal histogenesis have been examined. The first was the suggestion that the asymmetry was related to the emergence, during this period, of a binocular visual field secondary to the relative migration of the two eyes. It is shown that the asymmetric pattern of histogenesis is not closely related to those retinal areas that come to view binocular visual space. It was found, however, that the asymmetry of retinal growth from metamorphic climax was that required to stabilize retinal visual field positions with respect to body position. It is suggested that this minimizes the requirements for visuomotor readjustments that would otherwise be necessary to compensate for a situation in which eye position, relative to the body, is changing.

\* Present address: Department of Anatomy, Medical College of Pennsylvania, 3200 Henry Avenue, Philadelphia, Penn 19129, USA (MRC Studentship).

**Key words:** retina, optic tectum, histogenesis, amphibia, ocular migration, *Xenopus laevis*, autoradiography.

## INTRODUCTION

The amphibian retinotectal projection was established as a model on which to investigate the formation of ordered neuronal connections by the pioneering work of Sperry (1943, 1944, 1951). Many studies have observed the pattern of connections resulting from experimental perturbation of the developing or regenerating retinotectal system. The results have played a major part in shaping current views on factors regulating spatially ordered synaptogenesis (reviewed in Gaze, 1978; Jacobson, 1978; Edds, Gaze, Schneider & Irwin, 1979; Meyer, 1982; Gierer, 1983).

Studies of the normal maturation of the retinotectal system in larval *Xenopus laevis* produced results that have stimulated considerable interest. This work (Straznicky & Gaze, 1971, 1972; Gaze, Keating & Chung, 1974; Gaze, Keating, Ostberg & Chung, 1979) drew attention to the disparate modes of histogenesis in the retina and in the tectum during larval life. The retina grows by accretion of cells at a germinative zone at the ciliary margin. Tectal histogenesis, on the other hand, proceeds by the serial addition of strips of cells, this serial addition proceeding from ventrolateral to caudomedial tectum. A topographically ordered retinotectal projection exists from early larval life (Gaze *et al.* 1974; Holt & Harris, 1983) and functional synaptic connections are present (Scott, 1974; Chung, Keating & Bliss, 1974). Together these findings imply that larval maturation of the retinotectal projection involves ordered and systematic changes in retinotectal connections (Gaze *et al.* 1979).

During the later stages of metamorphic climax and in postmetamorphic life in *Xenopus*, changing skull shape causes relative migration of the two eyes (Fig. 1). This migration has two consequences. The coordinates of the monocular visual field of each eye change with respect to the coordinates of the body of the animal. The increasing overlap of the two monocular visual fields produces a steady enlargement of the binocular portion of the visual field.

We are interested in determining the response of the visual system in *Xenopus* to the problems posed by these changing interocular and visuomotor relationships. As part of this interest we required information on the details of changing eye position and on the modes of growth of the retina and optic tectum during this period. For example, Jacobson (1976) drew attention to the fact that in later larval life retinal histogenesis is asymmetric, much greater histogenesis occurring at the ventral retinal margin than dorsally. Beach & Jacobson (1979) suggested that the asymmetric pattern of accretion of retinal ganglion cells during this period may relate to the emergence of a binocular visual field at this time. We sought to examine this proposal by quantitative comparison of the pattern of retinal histogenesis and the emergence of the binocular visual field.

Retinal and tectal growth and histogenesis during metamorphosis and the postmetamorphic period were studied using tritiated thymidine autoradiography and morphometric methods. Changing eye position and the growth of the binocular visual field were measured by optical methods.

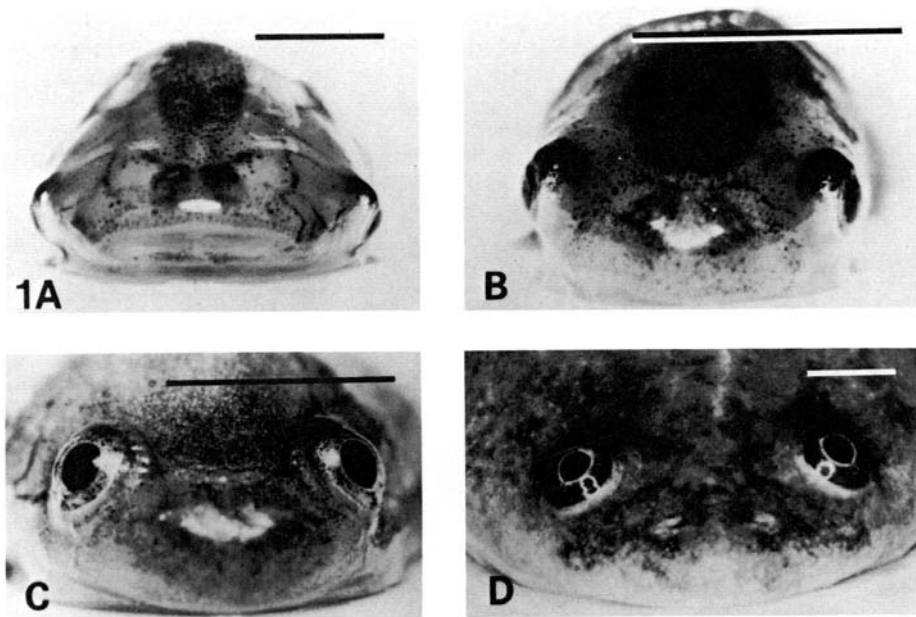


Fig. 1. Changing eye position with development in *Xenopus*. Frontal views of the head and eyes are shown for four developmental stages. (A) stage-58 tadpole; (B) stage 62; (C) two weeks after metamorphosis; (D) ten years after metamorphosis. Bars equal 5 mm.

## METHODS

The animals used in this study were raised in the laboratory from eggs obtained by injection of gonadotrophins into breeding pairs. Animals at various ages were anaesthetized with MS 222 (ethyl-m-aminobenzoate, Sigma) and received single intraperitoneal injections of methyl [ $^3\text{H}$ ]thymidine (Amersham International). Metamorphosing, juvenile (up to 1 year post-metamorphosis) and adult (10 years old) animals received 5  $\mu\text{Ci}$ , 10  $\mu\text{Ci}$  and 25  $\mu\text{Ci}$  respectively ( $1 \mu\text{Ci} \mu\text{l}^{-1}$ ; specific activity 42  $\text{Ci mmol}^{-1}$ ). The animals were allowed to survive for variable periods up to one year before decapitation under MS 222 anaesthesia.

In *Xenopus* metamorphosis begins at stage 49 (Nieuwkoop & Faber, 1967) with the emergence of limb buds. Metamorphosis is complete at stage 66. In this paper we use the term perimetamorphic to cover stages 58–66. The term early juvenile is used for the period 6–13 weeks after metamorphosis and late juvenile for the period 6–12 months after metamorphosis. The term adult covers animals aged 2 or more years postmetamorphosis.

## Histology

The heads were fixed in Bouin's solution for 24–72 h, depending upon the age at sacrifice, and then decalcified. The eyes were removed with the surrounding tissue intact to aid orientation for sectioning. One eye from each animal was sectioned in the vertical plane, the other in the horizontal plane. Brains were sectioned in horizontal, parasagittal or transverse planes. Dewaxed slides were dipped in K2 emulsion (Ilford). After exposure for 21 days the slides were developed in D19 developer (Kodak) and counterstained with Harris' haematoxylin.

## Morphometric analysis

### (1) Retina

Reconstruction of the retina, calculation of its surface area and the position of labelled cells in the retinal ganglion cell layer, utilized a digitizer pad linked to a minicomputer. Camera-lucida

drawings of every fifth retinal section (or every tenth section in the older animals) were made and the positions of labelled cells were marked, as were the positions of the ciliary margin. The overall retinal length was measured, as were the distances from labelled cells to the retinal periphery and the distance between the bands of labelled cells.

The retina, for reconstruction purposes, was assumed to form part of a spherical surface. The nasotemporal and dorsoventral diameters of the eye are equal as shown by *in vivo* measurement and from histological sections but the anteroposterior diameter is slightly less, so this assumption involves a small approximation. Our measurements, both of the visual field projection of the retinal reflection (see below) and of the meridional retinal sections indicate that the angular subtense of the retina is approximately  $200^\circ$ . If retinal reconstruction revealed that the plane of section had deviated significantly from that intended, data from those eyes were discarded. In the remaining eyes those sections containing the longest retinal lengths were regarded as meridional, the dorsoventral meridian in vertically sectioned eyes and the nasotemporal meridian in horizontally sectioned eyes. A great circle arc of  $200^\circ$ , of a sphere of radius  $r$ , has a length  $l$  given by

$$l = 2\pi r \times \frac{200}{360} = \frac{10\pi r}{9}.$$

The retinal radius was thus obtained from the mean meridional length of the two eyes from the formula

$$r = \frac{9l}{10\pi}.$$

The surface area ( $A$ ) of the portion of a sphere subtended by a solid angle  $2\alpha$  is given by the formula

$$A = 2\pi r^2(1 - \cos \alpha).$$

Since the retinal subtense is  $200^\circ$  the surface area of the retina is given by

$$A = 2\pi r^2(1 - \cos 100) = 7.35r^2.$$

Retinal reconstructions were made by the method of Gaze *et al.* (1979). The retina is represented as a circular planar surface which is the polar projection system in standard use for representing the monocular visual field in maps of the retinotectal projection. Each retinal section is represented as an arc on this projection; the position of the centre of the arc, and the radius of curvature of the arc depending upon the distance of the retinal section from the meridional section. The meridional section itself is situated on the corresponding meridional line (nasotemporal or dorsoventral) of the projection. Its radius of curvature is infinite.

Even with good planes of section there are difficulties in measuring and analysing sections at either retinal extremity. To avoid errors analysis was restricted to those 50% of sections distributed about the meridional section. 'Whole' retinal reconstructions for each animal were obtained by combining the results from the two eyes, one of which had been sectioned vertically, and the other horizontally.

The number of cells in the retinal ganglion cell layer were estimated by counting all nuclei in the median three to five sections in each retina. The number was corrected for split nuclei using Königsmark's (1970) modification of the Abercrombie (1946) method. From these figures and knowledge of the lengths of retina and of section thickness ( $10\mu\text{m}$ ) from which they had been obtained, the surface density of cells was obtained. Total ganglion cell numbers were obtained by multiplying the surface density by the surface area. This was permissible because surface density of ganglion cells is relatively uniform in *Xenopus* (our own observations and those of Graydon & Giorgi, 1984; Dunlop & Beazley, 1984).

## (2) Tectum

The size of the tectum at various ages was measured by three methods:

- (i) Three-dimensional reconstruction from histological sections.

(ii) *In vivo* measurements, by stereomicromanipulator, of the rostrocaudal and mediolateral tectal dimensions, accessible by a dorsal approach.

(iii) From enlarged photographs of the dorsal surface of the tectum *in vivo*.

All three methods were in accord as to the trends in tectal growth during the period under study. The histological method was, however, the most accurate since the marked curvature at the rostral and lateral aspects of the tectum was not easily quantified *in vivo*. The data on tectal growth in this paper derive from this histological method. Control experiments, in which lesions were placed at specified intervals in the tectal surface *in vivo*, indicated a 20 % linear shrinkage as occurring during histological fixation. The presented data for both tectal and retinal growth are corrected for this shrinkage.

The tectal surface is curved in three dimensions but approximates to an ellipse. This surface was represented on the plane in a projection which preserves the rostrocaudal and mediolateral linear relationships of the surface at the cost of slight areal distortions. The positions of labelled cells in layers 8 or 6 of the tectum were plotted on this tectal representation. The more caudal aspects of the 'optic' tectum are, in fact, non visual. Tritiated proline autoradiography shows that it receives no visual input (Udin & Keating, 1981, fig. 3). It does not contain neuronal layers 8 and 6. Electrophysiological mapping, and the placement of lesions at the most caudal region of the tectum from which visually evoked responses may be recorded, confirmed that the visuorecipient portion of the tectum is that containing layer 8 and a discrete layer 6 (Grant & Keating, in preparation). Our measurements of the growth of the optic tectum refer to the visuorecipient area of the tectum.

### (3) Tectal cell counts

Quantitative measures of cell number in layers 6 and 8 of the tectum were obtained from one animal at stage 66 and one animal at 1 year postmetamorphosis. In each animal cells in both tecta were counted. The brains were sectioned transversely and in every tenth section the nuclei in layers 8 and layer 6 were counted, corrected numbers being obtained by the modification of Konigsmark (1970). The thickness of layer 6 was measured but as layer 8 is rather diffuse in anurans the thickness of combined layers 9, 8 and 7 were measured, i.e. from the pial surface to the dorsal surface of layer 6. In one adult animal (body length 9.5 cm) more restricted observations were made and extrapolated to give 'total' cell counts.

### Optical measurement of the monocular and binocular visual fields

The extent of the monocular visual field, and of the overlap of the two monocular fields to produce a binocular field, were determined by reverse ophthalmoscopy using essentially the technique of Fite (1973) and Grobstein & Comer (1977). In brief, the edge of the retina is observed in the ophthalmoscope and its projection noted by reversing the ophthalmoscope. The optic axis is determined by ophthalmoscopically lining up the series of Purkinje images from cornea and lens and back-projecting this position. The projection of the optic nerve head, visualized by retinal transillumination, was also plotted. The accuracy of these methods, as indicated by the consistency of repeated observations was some 5°. Interobserver differences were seldom larger than this.

## RESULTS

### Body growth with age

*Xenopus* undergoes a considerable increase in body size from perimetamorphic climax to adult life. During this period body length, measured from nose to anus, increased from  $18 \pm 1.7$  mm ( $n = 33$ ) to  $94 \pm 10$  mm ( $n = 9$ ).

### Changes in eye position

At stage 58 of larval life the two eyes face laterally. As metamorphic climax proceeds changes in skull shape produce a dorsal and nasal migration of each eye.

This continues after metamorphosis (Fig. 1). Quantification of these changes with age was obtained by noting the position of the optic axis with respect to the planes of the animal's head. Parameters of this changing interocular geometry are given in Table 1. It may be seen from that Table that the distance between the two eyes reduces during the perimetamorphic period but then increases again with postmetamorphic growth. The reducing interocular angle, which is the angle between the two optic axes, is a measure of the frontal component of the eye migration. This angle reduces from  $161^\circ$  at stage 60 to  $51^\circ$  in adult life. The  $110^\circ$  decrease means that each eye migrates frontally by  $55^\circ$ . The angle of elevation of the optic axis with respect to the horizontal plane increases from  $0^\circ$  to  $50^\circ$ , reflecting the dorsalward component of eye migration between stage 60 and adult life.

One effect of this migration is that the two monocular visual fields overlap and the degree of overlap increases with age. By adulthood the binocular field is some  $150^\circ$  across. Following up a suggestion by Beach & Jacobson (1979) that the asymmetric pattern of histogenesis in later larval life may relate to the emergence of this binocular portion of the visual field we plotted the growth of the binocular field and compared it to the pattern of retinal histogenesis.

Ophthalmoscopic measurement of the monocular visual field of each eye indicated that it was symmetrically distributed around the optic axis of that eye and extended out from that axis some  $100^\circ$ . The binocular visual field can be plotted on various coordinate systems, the most obvious of which is a head-centred one. For purposes of comparison with retinal histogenesis, however, it is most convenient to plot the growth of the binocular visual field on a coordinate system centred on

Table 1. *Changes in interocular geometry with age*

Age	External ocular diameter (mm)	Interocular distance (mm)	Interocular angle (degrees)	Angle of elevation (degrees)
St 58	1.6	13.5	$181 \pm 15$ (n = 4)	$-15 \pm 4$ (n = 3)
St 60	$1.8 \pm 0.1$ (n = 2)	$8.5 \pm 0.9$ (n = 2)	161 (n = 2)	$0 \pm 2$ (n = 2)
St 62	$1.6 \pm 0.2$ (n = 7)	$6.1 \pm 0.7$ (n = 11)	$140 \pm 12$ (n = 6)	$12 \pm 2$ (n = 6)
St 64	$1.7 \pm 0.2$ (n = 12)	$4.6 \pm 0.2$ (n = 11)	$115 \pm 5$ (n = 6)	$17 \pm 3$ (n = 12)
St 66	$1.8 \pm 0.3$ (n = 9)	$4.9 \pm 0.3$ (n = 9)	$99 \pm 6$ (n = 7)	$21 \pm 3$ (n = 7)
Early juvenile	$2.2 \pm 0.2$ (n = 24)	$6.2 \pm 0.6$ (n = 24)	$76 \pm 5$ (n = 9)	$29 \pm 3$ (n = 22)
Late juvenile	$3.0 \pm 0.4$ (n = 16)	$8.5 \pm 0.9$ (n = 16)	$64 \pm 3$ (n = 5)	$37 \pm 4$ (n = 17)
Adult	$4.9 \pm 0.4$ (n = 9)	$15.2 \pm 1.1$ (n = 9)	$51 \pm 3$ (n = 5)	$50 \pm 4$ (n = 5)

the optic axis of one eye, since that is the coordinate system on which the histogenesis is plotted. Fig. 2 shows the growth of the binocular visual field with age. The edge of the monocular field of the left eye is shown on a coordinate system centred on the optic axis of the right eye. The boundaries of the disc thus represent the monocular field of the right eye. The binocular visual field is the area of overlap of the two monocular visual fields and occupies the nasosuperior portion of the visual field of the right eye.

### *Retinal growth*

Morphometric methods were used to study retinal growth and the pattern of histogenesis during the perimetamorphic and postmetamorphic period. From measurements on histological material it was found that the meridional length of the retina increases some four-fold (Fig. 3). The corresponding increase in retinal surface area is sixteen-fold. Table 2 summarizes data from animals at stage 64, at three months after metamorphosis, at twelve months after metamorphosis and, in a 10-year-old adult.

The number of cells in the ganglion cell layer quadruples during this period, but this is considerably less than the increase in retinal surface area. There is,

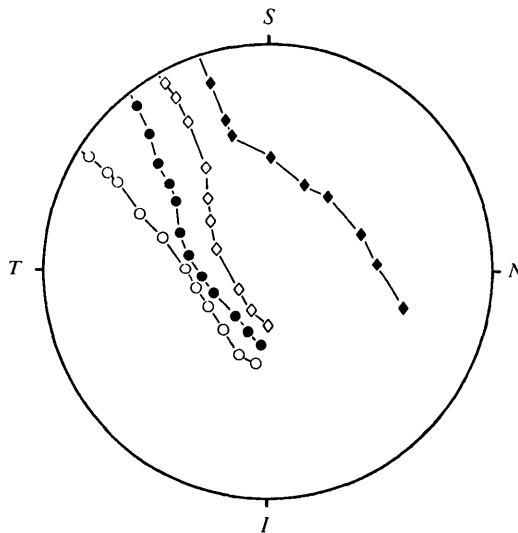


Fig. 2. Developmental changes in the extent of the binocular visual field. The optically determined nasal boundary of the visual field of the left eye is plotted on a coordinate system centred on the optic axis of the right eye. For technical reasons it was not possible, on this coordinate system, to plot accurately the nasoinferior portion of the boundary of the visual field of the left eye. On this coordinate system the binocular portion of the visual field is that portion between the nasal boundary of the field of the left eye and the nasosuperior periphery of the field of the right eye. The results are shown as mean results from animals at stage 62,  $\blacklozenge$  ( $n = 2$ ); stage 66,  $\diamond$  ( $n = 3$ ); three months after metamorphosis,  $\bullet$  ( $n = 3$ ); and one year after metamorphosis,  $\circ$  ( $n = 2$ ). N, T, S, I – nasal, temporal, superior and inferior poles of the visual field of the right eye. It may be seen that the binocular visual field increases in size with age.

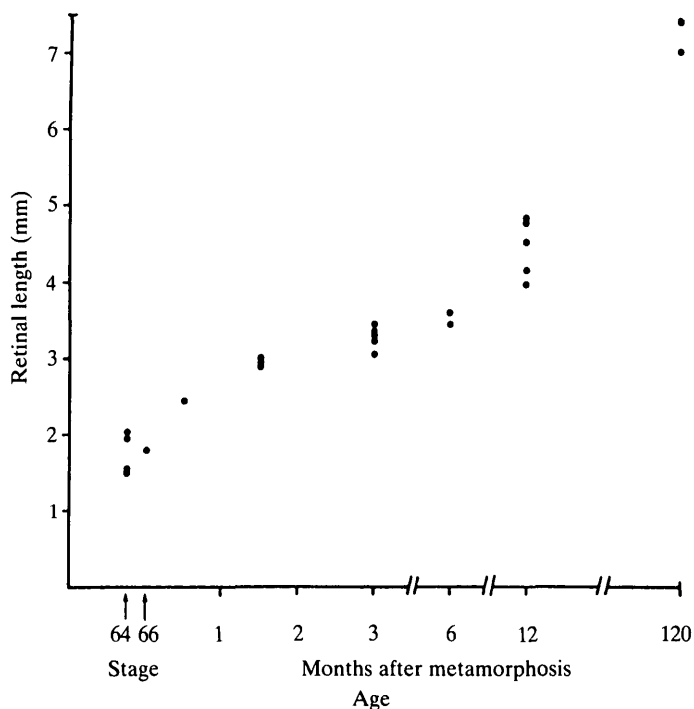


Fig. 3. A graph of the relationship between meridional retinal length and age. The length of the retina was measured along the ganglion cell layer. On the basis of comparison of *in vivo* and post-processing ocular diameters, an allowance of 20 % was made for tissue shrinkage during fixation.

therefore, a four-fold reduction in cell density in the retinal ganglion cell layer. This reduction is evident in Fig. 4 which also illustrates that the increase in retinal thickness with age is much less than growth in the other retinal dimensions. There is some thinning of the inner nuclear layer and an increase in the length of the receptor outer segments.

Table 2. *Changes in retinal size, ganglion cell density and ganglion cell number with age*

Age	Retinal length (mm)	Retinal surface area (mm <sup>2</sup> )	Mean ganglion cell number/section	Cell surface density (mm <sup>-2</sup> )	Total number of cells
St 64	1.76	1.88	260	11 800	22 200
3 MAM	3.28	6.48	344	8 400	54 600
12 MAM	4.30	11.18	301	5 600	62 600
Adult	7.20	32.12	259	2 800	91 400

MAM = months after metamorphosis.

The number of retinæ examined were  $n = 4$ , for St 64, 3 MAM, 12 MAM and  $n = 2$  for adult. Equal numbers of retinæ at each stage were sectioned vertically and horizontally. For each retina examined the mean ganglion cell number represented the mean of counts obtained from five sections distributed about the meridional section.



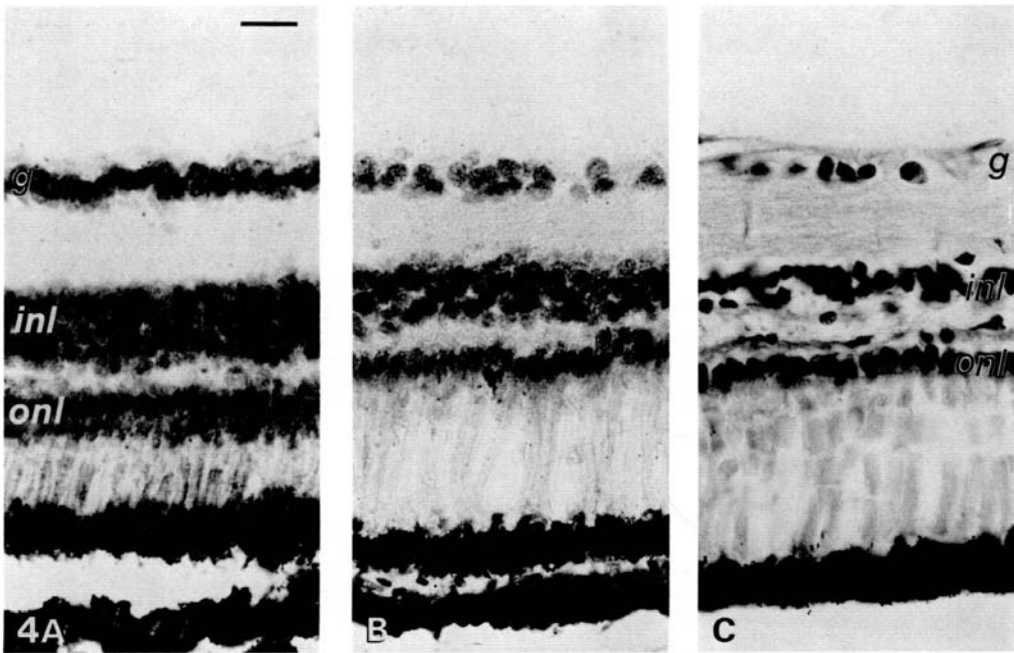


Fig. 4. Photomicrographs of horizontal sections of the retina, just ventral to the optic nerve head, from *Xenopus* aged stage 66 (A), three months postmetamorphosis (B) and adult (C). *g*, ganglion cell layer; *inl*, inner nuclear layer; *onl*, outer nuclear layer. Bar equals 20  $\mu\text{m}$ .

### Retinal histogenesis

Straznicky & Hiscock (1984) have recently described retinal histogenetic patterns in *Xenopus laevis* receiving pulses of tritiated thymidine at stage 58, 62 and 66 of larval life and examined at intervals up to 9 months after metamorphosis. In general terms our results are in broad agreement with theirs. They will, therefore, be presented only briefly. Our purpose in presenting this data is four-fold: (1) to provide baseline information for a comparison of the retinal histogenetic pattern with the growth of the retinal representation of the binocular visual field; (2) to supply further information on postmetamorphic retinal growth as revealed by pulses of tritiated thymidine administered postmetamorphically; (3) to point up one area of significant disagreement between our findings and those of Straznicky & Hiscock (1984) and (4) because analysis of our data has raised an unexpected issue regarding postmetamorphic retinal histogenesis.

Animals receiving a single pulse of [ $^3\text{H}$ ]thymidine at metamorphic or juvenile stages and examined at short survival times show label restricted to the ciliary margin of the retina (Fig. 5). This indicated that the ciliary margin continues to be the germinative zone for retinal histogenesis.

With longer survival times, the label occupied a circumscribed band, extending through all retinal layers, displaced some distance from the ciliary margin. Findings in an animal labelled at stage 66 and sacrificed six weeks after

metamorphosis are illustrated in Figs 6 and 7. Since the ciliary margin is the germinative zone the unlabelled cells peripheral to the labelled band have appeared since the time of label administration; those central to the labelled band were generated prior to label administration. Labelled cells of the nuclear layers are displaced centrally with respect to the position of labelled ganglion cells. This was a consistent feature of our autoradiographs. Figs 6 and 7 together indicate that in the period from stage 66 to six weeks postmetamorphosis histogenetic growth is greatest at the ventral margin, is slightly greater at the temporal margin than at the nasal margin and no histogenesis was observed at the dorsal margin.

Fig. 7B illustrates the rare observation of labelling in a central retinal region. A group of cells are labelled in the inner nuclear layer and an adjacent labelled cell is seen in the ganglion cell layer.

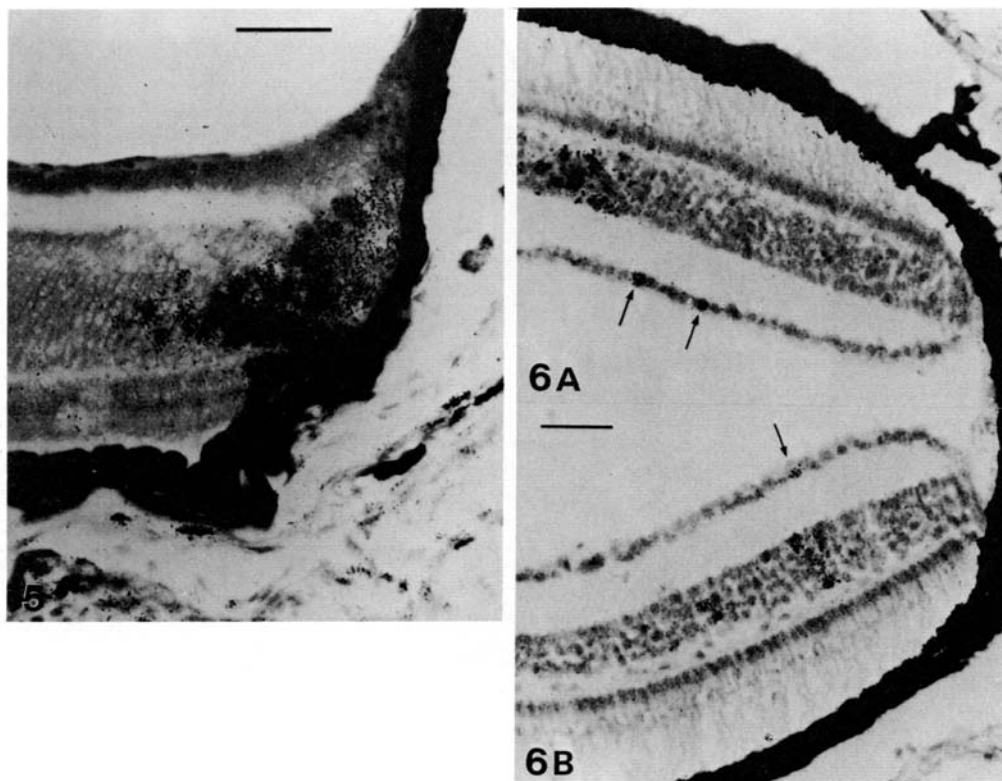


Fig. 5. Autoradiograph of the ventral retinal margin of a stage-64 *Xenopus* injected with [ $^3\text{H}$ ]thymidine at stage 62 (survival time, 48 h). A number of nuclei in the germinative zone have incorporated label and are overlaid with silver grains. Some labelled cells in the inner nuclear layer are slightly displaced from the margin. Bar equals 20  $\mu\text{m}$ .

Fig. 6. Autoradiographs of the temporal (above) and nasal (below) retinal poles from a 6-week postmetamorphic *Xenopus* injected with [ $^3\text{H}$ ]thymidine at metamorphic climax (stage 66). Arrows indicate the positions of labelled ganglion cells. The number of labelled cells and their displacement from the periphery are greater at the temporal pole. Bar equals 40  $\mu\text{m}$ .

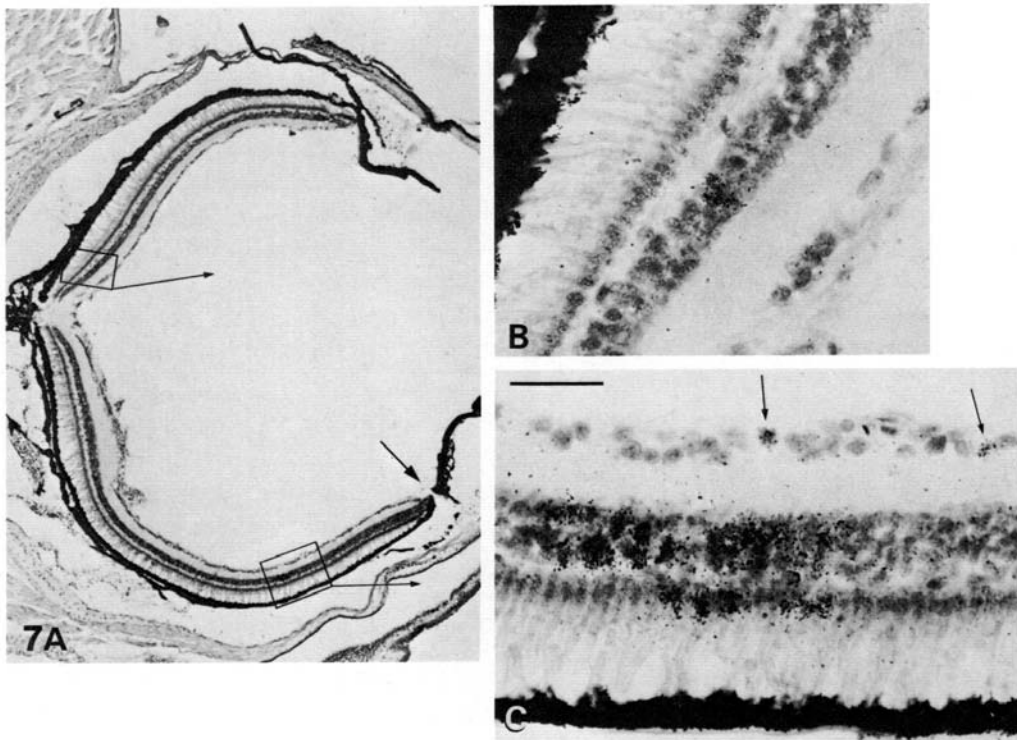


Fig. 7. Autoradiographs of the retina of a 6-week postmetamorphic *Xenopus* injected with [ $^3\text{H}$ ]thymidine at metamorphic climax (stage 66). (A) Vertical section through the optic nerve head. Dorsal is uppermost and the entry of the ophthalmic blood vessels at the ventral retinal pole is indicated by the arrow. No labelled cells were found at the dorsal pole. Enlargements show (B) some labelled cells in the inner nuclear layer and ganglion cell layer just dorsal to the optic nerve head; (C) label in the cell layers of the ventral retina displaced some distance from the ventral pole. Arrows indicate the positions of labelled cells in the ganglion cell layer. Bars equal (A) 267  $\mu\text{m}$ ; (B) and (C) 40  $\mu\text{m}$ .

An overview of the pattern of retinal histogenesis during the perimetamorphic and juvenile period was obtained by plotting the positions of the labelled ganglion cells on representations of the reconstructed retina (see Methods). The results from several animals receiving [ $^3\text{H}$ ]thymidine at different perimetamorphic and postmetamorphic stages are pooled in Fig. 8. The disc represents the retina at one year postmetamorphosis and the positions of ganglion cells labelled at different stages are indicated on the Figure.

The rate of histogenetic activity at the ciliary margin and, hence, the addition of new peripheral retina decreases markedly during this period. The proportions of new retina being added between different stages may be calculated from representations such as those of Fig. 8. Table 3 indicates the proportions of the retina existing one year after metamorphosis which were produced at various developmental intervals. It may be seen that, of the retina existing one year after metamorphosis, 30 % was produced after stage 62, but only 4 % of the retina was

produced after three months postmetamorphosis and less than 1 % was produced after six months postmetamorphosis. Adult animals receiving a single pulse of [ $^3\text{H}$ ]thymidine showed no retinal labelling.

*Retinal histogenesis and the binocular visual field*

Fig. 8 reveals the pattern of retinal histogenetic activity during the perimetamorphic and postmetamorphic period. In Fig. 2 was shown, on right-eye centred coordinates, the growth of the binocular portion of the visual field. The area of the right retina viewing the binocular visual field may be obtained by camera inversion of Fig. 2. In Fig. 9, the area of retina that views the binocular visual field that appears between stage 62 and one year postmetamorphosis, is compared with the pattern of retinal histogenesis between these ages. It can be seen that there is no good correlation between 'new' retina and retina viewing the binocular visual field. Thus, some of the 'new' retina, the nasosuperior periphery, does not view binocular visual space. Conversely, a considerable portion of the 'new' binocular visual field is viewed by 'old' retina.

*Asymmetrical retinal histogenesis and the visual field projection of the optic nerve head*

If there is no obvious correlation between asymmetrical retinal histogenesis in the perimetamorphic and postmetamorphic period and the emergence of a

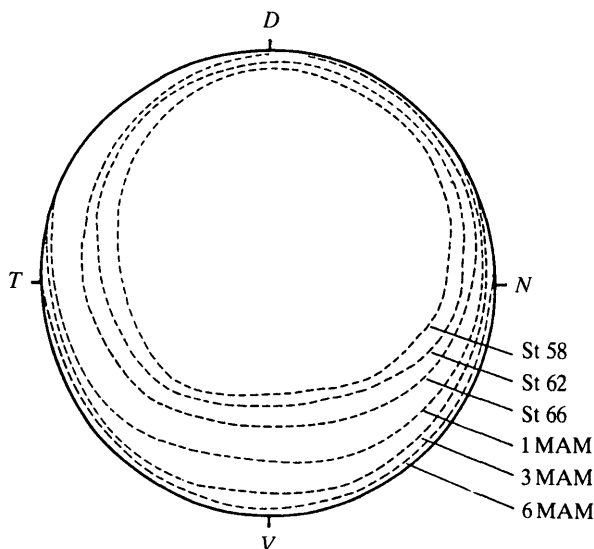


Fig. 8. Reconstructions of retinal histogenetic growth patterns in the perimetamorphic and juvenile period. Retinae were reconstructed and represented on circular discs. The positions of the labelled ganglion cells are plotted on the representation of the retina at one year after metamorphosis. This figure contains pooled results from animals receiving a single pulse of [ $^3\text{H}$ ]thymidine at stage 58, stage 62, stage 66, one month, three months, and six months after metamorphosis and sacrificed one year after metamorphosis. N, T, D, V – nasal, temporal, dorsal and ventral poles of the retina. MAM = months after metamorphosis.

Table 3. *Percentage of retinal area existing in 1 year postmetamorphic animal produced between different developmental stages*

Age	% of retina at 1 year, produced during interval shown
St 58 – 1 year	39
St 62 – 1 year	31
St 64 – 1 year	29
St 66 – 1 year	21
2–6 WAM – 1 year	11
3 MAM – 1 year	4
6 MAM – 1 year	<1

WAM, MAM = weeks, months after metamorphosis.

binocular visual field, is there any link between such a pattern of retinal histogenesis and a second consequence of changing eye position? The frontal and dorsal migration of the eye produces a continuous alteration in the relationship between the coordinates of the monocular visual field and those of the body. If retinal growth during this period were purely symmetrical, the receptive field position of any retinal ganglion cell would undergo corresponding changes with respect to a body-centred coordinate scheme. This would presumably require a continuous readjustment of the integration of visual information with body-based motor and somatosensory systems. It occurred to us that the asymmetric mode of retinal growth might serve to minimize any such readjustments.

The oldest retinal ganglion cells are those in the region of the optic nerve head (Straznicky & Gaze, 1971). We examined the visual field projection of the optic nerve head, with respect to the optic axis, at various perimetamorphic and postmetamorphic stages. The results are presented in Table 4 and illustrated in Fig. 10. In larval life the optic nerve head is in ventral retina. The asymmetric retinal growth produces a progressive dorsal displacement of the optic nerve head within the retina. At stage 62 the projection of the optic nerve head coincides with the optic axis. Thereafter there is a progressive displacement of the projection of the optic nerve head into the ventrotemporal quadrant of the visual field (Fig. 10). This corresponds to a progressive displacement of the optic nerve head into the dorsonasal retinal quadrant.

Quantification of the dorsoventral and nasotemporal components of this displacement is given in Table 4. From this Table it may be noted that between stage 66 and adulthood the projection of the optic nerve head, with respect to the optic axis is displaced 25° ventrally and 19° temporally. Table 1 shows that, during this period, the optic axis moves 29° dorsally and 24° nasally, with respect to body coordinates. The dorsonasal retinal displacement of the optic nerve head from stage 66 onwards thus produces a ventrotemporal displacement of the projection of the optic nerve head which counters the dorsonasal migration of the eyes. These figures indicate that the visual field projection of the optic nerve head, and hence the receptive fields of the old retinal ganglion cells, remain constant with respect

to body coordinates despite the migration of the eyes. This is illustrated in Fig. 11 in which is shown, on body-centred coordinates, firstly the eye migration as indicated by the progressive dorsonasal movement of the projection of the optic

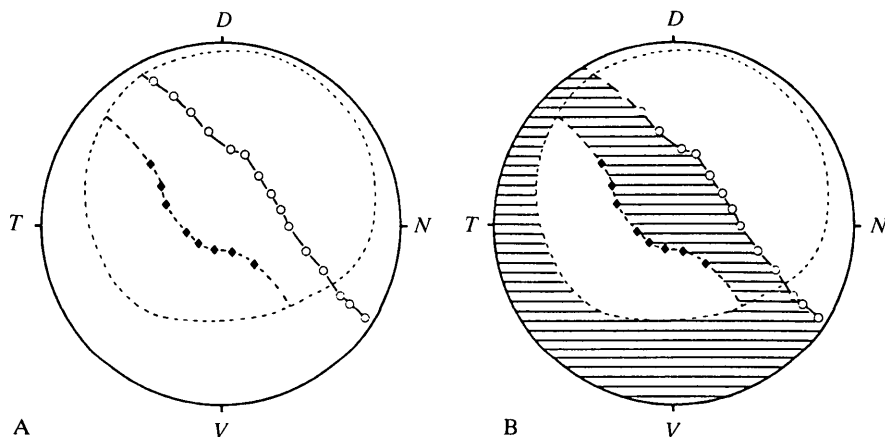


Fig. 9. Comparison of the pattern of retinal histogenesis from stage 62 to one year after metamorphosis with the growth of the binocular visual field during this period. (A) The circular disc represents the right retina at one year after metamorphosis, conventions as in Fig. 8. The fine interrupted line represents the position of retinal ganglion cells labelled by a single pulse of [ $^3\text{H}$ ]thymidine at stage 62, also taken from Fig. 8. The thick line joining the  $\bigcirc$  represents the retinal position in the right eye which 'views' the nasal boundary of the visual field of the left eye at one year after metamorphosis. This line is obtained by camera inversion of the corresponding boundary in Fig. 2, plus extrapolation of that line to the retinal boundary. At one year after metamorphosis, therefore, the portion of the right retina viewing the binocular visual field is the ventrotemporal retinal area bounded by the above line and the margins of the retinal disc.

To obtain that area of the right retina at one year postmetamorphosis which was viewing the binocular visual field at stage 62 was slightly more complicated. Fig. 2 indicates the boundary of the binocular visual field  $\blacklozenge$  plotted in a stage-62 animal. The portion of the stage-62 right retina that views this binocular portion of the visual field is obtained by simple camera inversion. In the one year postmetamorphic retina this portion of the stage-62 retina lies within the area defined by the fine interrupted line, since this represents retina present at stage 62. The thicker line joining the  $\blacklozenge$  represents the position in the one year postmetamorphic retina of that portion of the stage-62 retina which was then viewing the nasal boundary of the visual field of the left eye. The calculations underlying the determination of this line in the one year retina utilized the meridional equidistant feature of the polar equidistant azimuthal projection that is used to represent the retina and the visual field. They also assumed that retinal growth within this area, between stage 62 and one year postmetamorphosis, was uniformly hypertrophic. On this basis the portion of the retina at one year postmetamorphosis which was, at stage 62, viewing the binocular visual field is that contained in the ventrotemporal retinal area bounded by the interrupted fine line and the thicker line joining the  $\blacklozenge$ .

(B) Conventions as in Fig. 9A. The retinal representation of the growth in the binocular visual field that took place between stage 62 and one year after metamorphosis is shown at hatched. The 'new' retina that appears by histogenetic activity between stage 62 and one year after metamorphosis is the retina peripheral to the fine interrupted line.

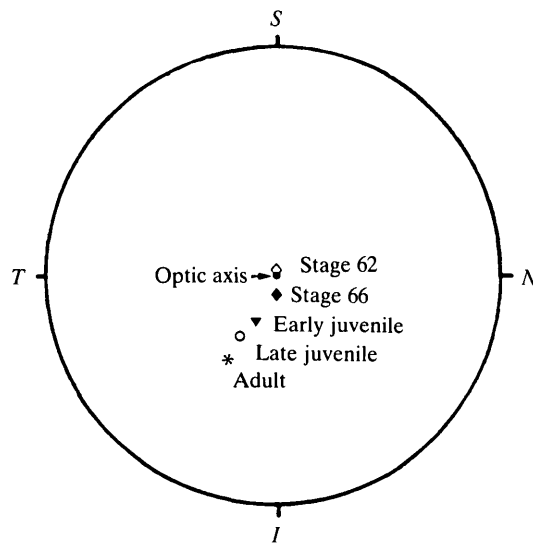


Fig. 10. The mean position of the projection of the optic nerve head on eye-centred coordinates at different peri- and postmetamorphic ages. The circle represents a polar projection of the visual field of the right eye with the optic axis of that eye centred on the origin of the polar system. It may be seen that from stage 62 to adult life there is a progressive ventral and temporal displacement of the projection of the optic nerve head with respect to the optic axis. *N, S, T, I* – nasal, superior, temporal, inferior poles of the visual field of the right eye.

axis (Fig. 11A) and secondly, the fact that from stage 66 onwards the visual field projection of the optic nerve head remains constant (Fig. 11B).

#### *Tectal growth*

There is little published information on perimetamorphic and postmetamorphic growth of the optic tectum in *Xenopus*. Straznicky & Gaze (1972), in their

Table 4. *Visual field projection of the optic nerve head with respect to the optic axis*

Age	Dorsoventral	Nasotemporal
Stage 62 (n = 7)	2° dorsal (±2°)	0°
Stage 66 (n = 6)	10° ventral (±2°)	0° (±3°)
Early juvenile (n = 6)	19° ventral (±4°)	13° temporal (±3°)
Late juvenile (n = 9)	26° ventral (±4°)	16° temporal (±4°)
Adult (n = 7)	35° ventral (±3°)	19° temporal (±4°)

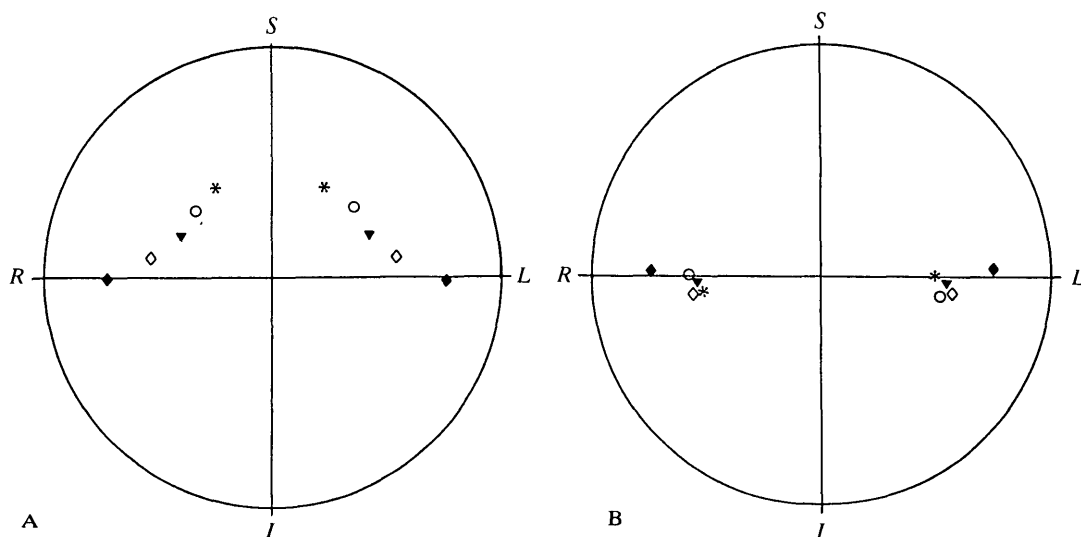


Fig. 11. The visual field projection of (A) the optic axes of the two eyes and (B) the optic nerve head in animals of different ages. Animals were placed at the centre of the projection apparatus. The sagittal axis of the animal was aligned with the vertical meridian of the projection system. The horizontal meridional plane of the projection system was fixed at an angle of  $10^\circ$  above that of the animal's horizontal plane. The different symbols represent data from animals at stage 62, ◆; stage 66, ◇; 6 weeks after metamorphosis, ▼; one year after metamorphosis, ○; and adulthood, \*. It may be seen that the optic axes of the two eyes move frontally and dorsally during this period. From stage 66 onwards, however, the projection of the optic nerve head is constant. S, I, R, L – superior, inferior, right and left aspects of visual field.

definitive study on tectal histogenesis during larval life, described the major features of this process. Based on the administration of tritiated thymidine between developmental stages 27–58, they concluded that tectal histogenesis occurred in waves proceeding from ventrolateral to caudomedial tectum, and that this phase of tectal histogenesis was essentially complete by stage 55. However, in animals receiving tritiated thymidine at stage 58, and in one animal labelled one month after metamorphosis and sampled 24 h later, Straznicky & Gaze noted a small number of labelled cells. It was possible that continued replication of a small number of cells over a protracted time period would make a significant contribution to the adult tectum, since this is exactly what happens in the retina.

We, therefore, undertook to quantify tectal growth in perimetamorphic and postmetamorphic *Xenopus* and to check whether any significant histogenesis was occurring during this period. The size of the tectal surface devoted to the representation of the visual field (for the distinction between this and the tectal surface itself, see Methods) was measured in 22 animals aged from stage 60 to adulthood. The rostrocaudal and mediolateral tectal lengths are plotted against age in Fig. 12. The mediolateral length exceeds the rostrocaudal length at all stages, the mean ratio between the two being 1.23. During this period tectal axial length increases by some 33 % and the surface area by some 80 %.



*Tectal histogenesis*

The incidence and distribution of all labelled cells in the tectum were studied at various intervals after administration of a single pulse of [ $^3\text{H}$ ]thymidine at one of the following ages, stage 58, 62, 64, 66, one month, three months or six months after metamorphosis. Tectal cell labelling was extremely sparse at all developmental stages examined, this being in marked contrast to retinal labelling in the same animals, and indeed to heavy telencephalic labelling seen in the same brain. Every tectal section was examined carefully for labelled cells.

The majority of observed labelled cells were seen in the ventricular and periventricular layers but a small number were seen in layers 6 and 8 (Fig. 13), the visuorecipient layers (Chung, Bliss & Keating, 1974). Counts of these latter were made and their positions within the tectum were noted. Three animals receiving a pulse of [ $^3\text{H}$ ]thymidine at stage 62/64 and killed 48 h later at stages 64/66 had a mean number (per tectum) of  $23 \pm 7$  labelled cells in the visuorecipient layers. Four animals received [ $^3\text{H}$ ]thymidine at stage 66 and were examined at either six weeks or three months after metamorphosis. The eight tecta showed a mean number of  $3 \pm 2$  labelled cells in the visuorecipient layers. For each of these two groups of animals the results were pooled and the tectal positions of the labelled

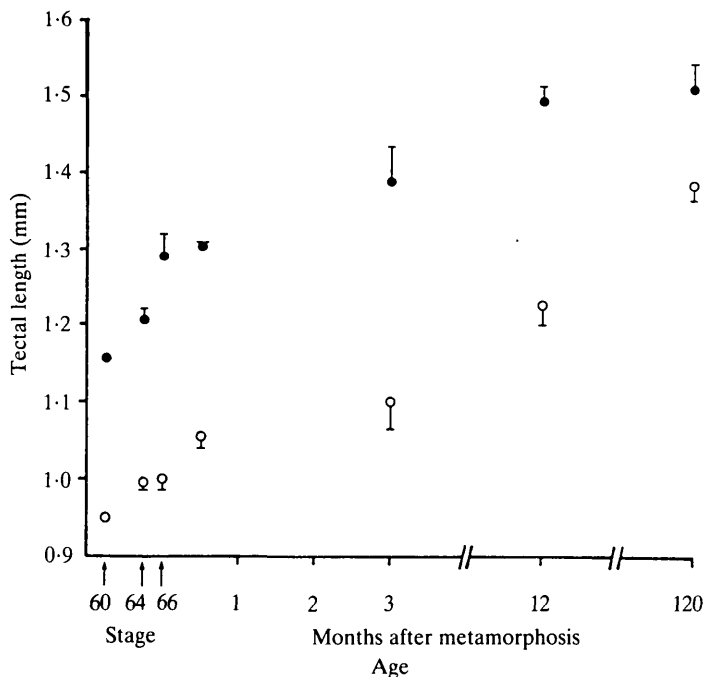


Fig. 12. A graph of tectal linear dimensions as a function of age. The point at each age represents the mean value. Standard deviation bars are shown unless they were smaller than the size of the symbol. The number of tecta measured for each stage were: stage 60 (2), stage 64 (8), stage 66 (4), 2 WAM (4), 3 MAM (8), 12 MAM (8), 120 MAM (4). WAM, weeks after metamorphosis; MAM, months after metamorphosis. ○, Rostrocaudal length; ●, mediolateral length.

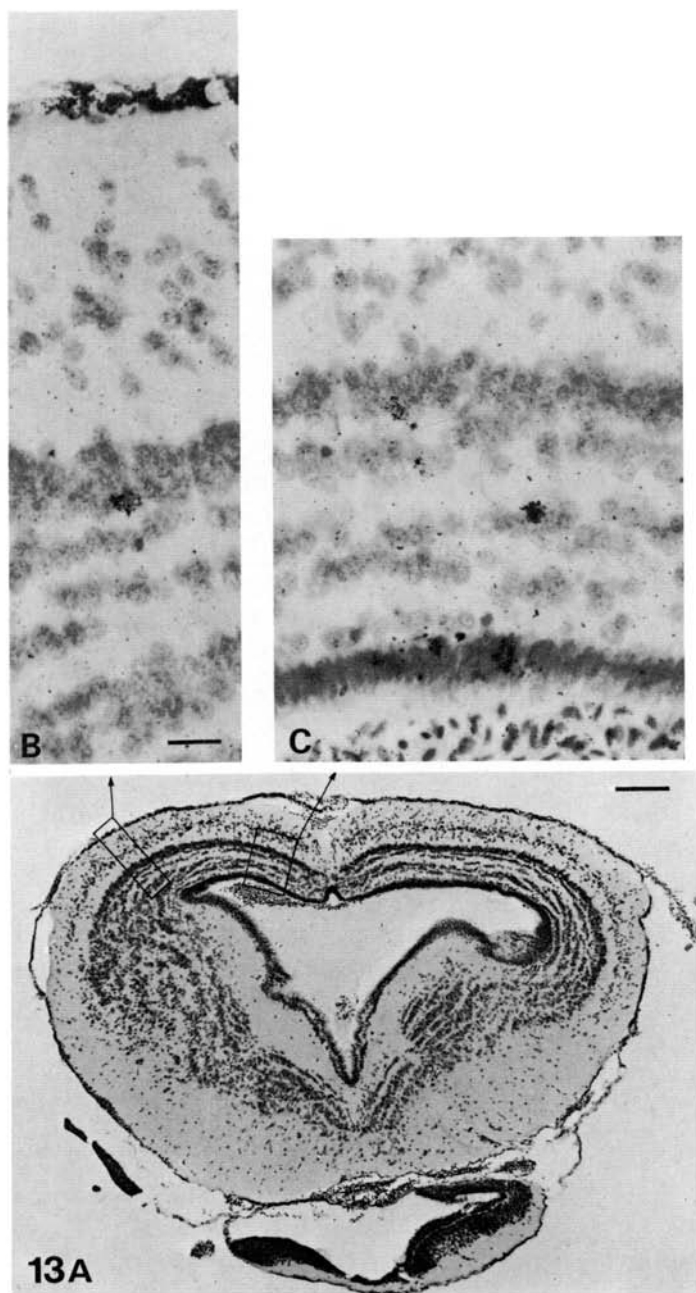


Fig. 13. Autoradiographs of a transverse section through mid-rostral tectum of a six week postmetamorphic *Xenopus*. The animal received a pulse of [ $^3\text{H}$ ]thymidine at stage 62. Labelled cells were found in the ependymal layer and in cell layers 4, 5 and 6 of the right tectum. In this animal no labelled cells were seen in the left tectum. Bar equals (A) 200  $\mu\text{m}$ ; (B) and (C) 20  $\mu\text{m}$ .

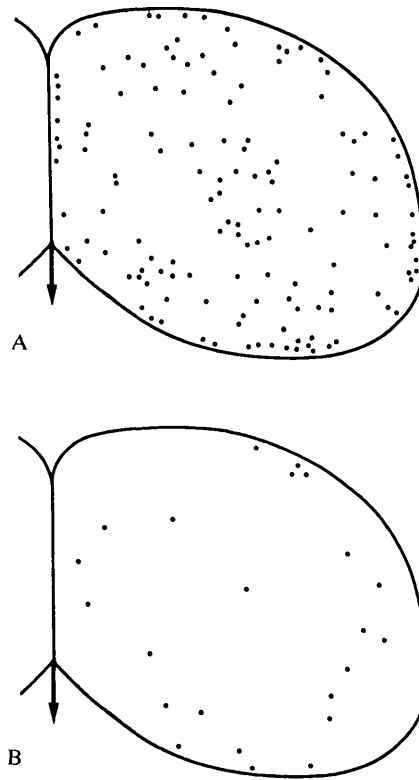


Fig. 14. The distribution of labelled cells in the tectum. Pooled data from (A) six tecta in animals at stage-64/66 labelled 48 h earlier, (B) eight tecta in animals aged 3 months after metamorphosis labelled at stage 66 or two weeks after metamorphosis. The midline arrow indicates rostral.

cells were plotted (Fig. 14). The distribution of labelled cells at metamorphic climax (Fig. 14A) seems quite unsystematic. For the early juveniles (Fig. 14B) there seems a slight tendency for the labelled cells to be distributed nearer to the periphery of the tectum rather than to its centre. There was, however, little consistency between animals and the histogenesis is so sparse that no obvious pattern is evident.

Our conclusion from this data is that little systematic or significant tectal histogenesis occurs postmetamorphically, certainly insofar as layers 6 and 8 are concerned. In order to check this conclusion estimates of total cell number in the visuorecipient layers were made in one animal at stage 66, in one late juvenile and in one adult (see Methods). The results are summarized in Table 5. Given the approximations made in the calculations we conclude that there is little change postmetamorphically in cell numbers in tectal layers 6 and 8.

If this conclusion regarding tectal histogenesis is correct, then the increase in tectal size postmetamorphically is hypertrophic. Table 5 contains data on the increase in volume in layers 6 and 8 (see Methods). The increase in volume of layer 6 was entirely accountable by the increase in cell volume in this period (assuming

cell volume is proportional to nuclear volume). In the more superficial layers, however, the greater part of the volume increase was due to increases in the fibre layers, particularly layer 9. Cell density decreased in inverse proportion to the volume increase.

To determine whether the postmetamorphic tectal hypertrophy was uniformly distributed, cell densities in rostral, mid and caudal tectum were compared in the stage-66 animal and in the one year postmetamorphic animal. This approach indicated that while the tectal hypertrophy was broadly uniform there was slightly greater hypertrophy in caudal as opposed to other tectal areas.

#### *The tectal representation of the optic axis and the optic nerve head*

In an earlier section we presented evidence that from stage 66 to adulthood, the visual field projection of the optic nerve head remains constant with respect to body-centred coordinates. We suggested that this minimizes the need for visuosomatic and visuomotor readjustments. Nevertheless the fact that retinal histogenesis is occurring in the earlier stages of this period, while tectal histogenesis apparently is not, implies the readjustment of retinotectal synaptic relationships. Electrophysiological mapping of the direct visuotectal projection (Grant & Keating, in preparation) at various stages during this period permitted us to determine the tectal representation of the ganglion cells in the vicinity of the optic nerve head. The results are shown in Fig. 15. The tectal representation of the optic nerve head is displaced caudolaterally.

## DISCUSSION

Marked changes in eye position take place in perimetamorphic and postmetamorphic life in *Xenopus laevis*. The alterations in interocular and visuosomatic relationships present difficulties for neuronal systems dealing with binocular integration, multimodality sensory integration and visuomotor programmes. As a first step in the investigation of how the central nervous system responds to these difficulties we report here the perimetamorphic and postmetamorphic patterns of

Table 5. *Changes in cell number, cell density and volume of the superficial tectal layers between metamorphosis, late juvenile and adult life*

Age	Layer 6			Layers 7, 8 and 9		
	Cell number	Volume ((10 $\mu$ m) <sup>3</sup> )	Cell density (cells (10 $\mu$ m) <sup>-3</sup> )	Cell number	Volume ((10 $\mu$ m) <sup>3</sup> )	Cell density (cells (10 $\mu$ m) <sup>-3</sup> )
Stage 66	29 000	17 500	1.66	27 500	94 500	0.28
1 year post-metamorphosis	32 000	22 600	1.28	27 900	187 800	0.14
Adult (10 years old)	30 400	31 200	0.95	29 400	367 000	0.08

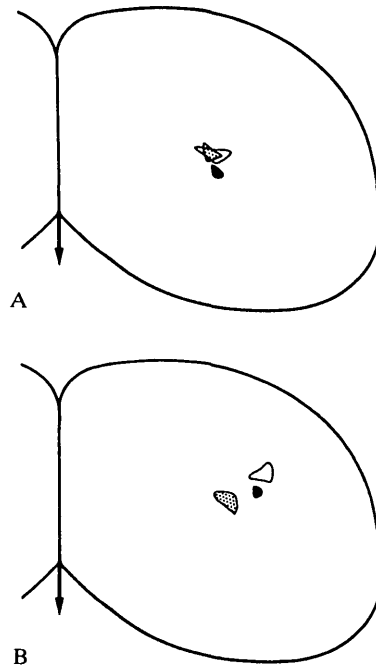


Fig. 15. The tectal projections of (A) the region of the optic axis and (B) the optic nerve head in animals of different developmental ages. The data derived from detailed electrophysiological maps of the contralateral visuotectal projection in animals, of various developmental ages, in which the visual field projection of the optic nerve head had been plotted. The tectal site of the projection of the optic nerve head was plotted. For purposes of comparison of the projection sites at different ages, the sites are presented on a 'standard' tectum. This latter was obtained by histological reconstruction of the entire tectal surface including the sharply curved rostral and lateral edges. These reconstructions were converted to a planar representation which preserves linear dimensions along the rostrocaudal and mediolateral dimensions. To adjust for the different sizes of tecta between stage 66 and adulthood it was assumed that tectal growth was by linear hypertrophy. The enclosed areas show the range of tectal projection sites in four animals at stage 66 (dotted area), four late juveniles (filled area) and five adults (open area).

growth and histogenesis in the retina and optic tectum. We consider the relevance of such patterns to the process of ocular migration.

Our autoradiographic studies indicate that retinal histogenesis is taking place until at least six months after metamorphosis. As in premetamorphic stages histogenesis is evident at the ciliary margin of the retina, but the rate of histogenesis decreases during the early juvenile period. Nevertheless some 30 % of the retina present one year after metamorphosis was produced after stage 62. The spatial pattern of the histogenesis during the postmetamorphic period showed the same asymmetry as that previously described for the premetamorphic period (Straznicky & Gaze, 1971; Hollyfield, 1971; Jacobson, 1976; Gaze, Keating,

Ostberg & Chung, 1979; Beach & Jacobson, 1979). There is considerable ventral histogenesis but virtually none at the dorsal retinal margin. There is also a temporonasal histogenetic asymmetry – temporal histogenesis being greater than nasal. Tay, Hiscock & Straznicky (1982) noted a similar asymmetry during the first two months after metamorphosis. There is, however, a conflict between our findings and those of Straznicky & Hiscock (1984) with respect to the retinal position of the optic nerve head in juveniles older than 2 months post-metamorphosis. Our data suggest a small but continuing displacement into nasal retina. Straznicky & Hiscock (1984), on the other hand, state that between 2 and 12 months postmetamorphosis the optic nerve head becomes displaced from the dorsonasal to the dorsotemporal retinal quadrant. The reason for this discrepancy is not clear. Straznicky & Hiscock's findings are based on retinal reconstructions whereas our data are based on optical measurements with the eye *in situ*. Conclusions, in this respect, deriving from retinal reconstructions are critically dependent upon the accuracy of the plane of sectioning. A small error in the plane of sectioning could result in the apparent transposition of a nasally placed optic nerve head into temporal retina. If Straznicky & Hiscock's data were correct the period between 2 and 12 months after metamorphosis would involve a 20° temporal shift in the position of the optic nerve head. During this period the dorsal shift is only some 5°. This implies that nasal retinal growth during this period is four times greater than ventral retinal growth. Such an asymmetry is not described by Straznicky & Hiscock and our histogenetic studies between 2 and 12 months after metamorphosis show no such asymmetry.

Tectal histogenesis in the postmetamorphic period has not previously been studied in *Xenopus*. In their pioneering study, Straznicky & Gaze (1972) noted a marked reduction in tectal histogenesis in late larval life. Our results extend their findings and support their conclusion that tectal histogenesis during the perimetamorphic and postmetamorphic period is minimal. The situation is somewhat different in adult goldfish. Meyer (1978) and Raymond & Easter (1983) describe a germinative zone around the caudal tectal rim in adult goldfish. The latter workers provided ultrastructural evidence that some of the progeny of the germinative zone were neuronal and counts showed that the periventricular layer of large (older) goldfish contained 27% more neurones than that of small goldfish. Following tritiated thymidine autoradiography in adult goldfish some labelled cells were seen in more superficial tectal layers (Meyer, 1978) but both Stevenson & Yoon (1981) and Raymond & Easter (1983) argued, on ultrastructural grounds, that these cells were glial. We do not know whether the labelled cells seen in the postmetamorphic tectum of *Xenopus* are neurones or glia.

Despite the very sparse histogenesis in the perimetamorphic and postmetamorphic period, the tectum in *Xenopus* increases in size, both in surface area and in thickness. In layer 6 this increase in volume is almost entirely due to growth in cell soma size. In layers 7, 8 and 9 on the other hand, a dominant feature of the hypertrophy is increase in thickness of the layers. This reflects primarily an increase in the volume of neuropil. These hypertrophic components are fairly

uniformly distributed across the entire tectum although cell density counts from different tectal regions at different ages do indicate a slightly greater hypertrophy in caudal tectum as opposed to rostral tectum.

We were interested in the possible relationship between developmental changes in eye position and asymmetric retinal histogenesis. One consequence of this ocular migration is to produce a progressively greater overlap of the two monocular visual fields such that more and more of the visual field in front of and above the animal is seen binocularly. A system of intertectal neuronal connections links the two optic tecta and is involved in the integration of visual information from binocular visual space. The changing geometry of the two eyes would seem to require a continuous readjustment of these intertectal connections (Keating, 1974; Grobstein & Comer, 1977). Beach & Jacobson (1979), however, put forward the intriguing proposal that perhaps the asymmetric retinal histogenesis might relate to the emergence of the binocular visual field and serve to minimize the readjustments of intertectal neuronal connections otherwise required. We have shown (Fig. 9) that the portion of retina that comes to view the binocular visual field shows little relation to the production of histogenetically new retina in this period. We report, elsewhere, (Grant & Keating, 1981, 1985) that the pattern of intertectal connections does indeed undergo dramatic readjustments with the emergence and enlargement of the binocular visual field.

The asymmetric pattern of retinal histogenesis does not seem, therefore, to relate closely to the emergence of a binocular visual field. Nevertheless, there is a sense in which Beach & Jacobson's proposal was a very perceptive one. Part of their proposal was that the asymmetric pattern could compensate for ocular migration with the result that old retina would continue to view constant regions of body-centred visual space. Our observations (Fig. 11) that from stage 66 onwards the projection of the optic nerve head, in body-centred coordinates, remains constant despite the dorsonasal movement of the eyes support this. The predominance of ventrotemporal histogenesis seems to be that required to compensate for dorsonasal ocular migration. We suggest that a rationale for the asymmetric histogenesis lies in this second consequence of ocular migration. The second consequence is that of changing the geometrical relationship between ocular coordinates and body-centred coordinates. In the absence of any compensation this change would present problems for visuomotor coordination, since a given locus on the retina would represent a series of different locations on body-centred space, this latter presumably forming the basis of the animal's motor map. The asymmetric retinal histogenesis minimizes this problem following the emergence of the mature body pattern. Thus, from at least stage 66 onwards the older portion of the retina, whilst its ocular coordinates change, looks at constant regions of body-centred space. Much less visuomotor readjustment is, therefore, required than would be the case if the histogenesis were not of the asymmetric kind that is observed.

It perhaps deserves emphasizing that some visuomotor readjustments are still required. One such requirement derives from the disparate modes of retinal and

tectal histogenesis. The demonstration that in larval *Xenopus* the modes of retinal and tectal histogenesis are geometrically disparate led to the proposal that retinotectal maturation involves a continuous adjustment and remodelling of retinotectal synaptic relationships (Gaze, Chung & Keating, 1972; Gaze *et al.* 1974). This idea was at first controversial (Jacobson, 1977). Evidence in its favour has, however, accumulated and data supporting the concept of shifting retinotectal connections have been obtained in larval *Xenopus* (Scott & Lazar, 1976; Longley, 1978; Gaze *et al.* 1979; Fraser, 1983), in larval *Rana* (Reh & Constantine-Paton, 1983, 1984) and in adult goldfish (Meyer, 1978; Marotte, 1980; Cook, Rankin & Stevens, 1983; Raymond & Easter, 1983; Easter & Stuermer, 1984). That this process occurs in juvenile *Xenopus* is indicated by our data. Dunlop & Beazely (1984) and Straznický & Hiscock (1984), on the basis of their studies on retinal growth in juvenile *Xenopus*, also argued that their findings implied shifting retinotectal connections. We show (Fig. 15) that one manifestation of these changing retinotectal connections in postmetamorphic life is the changing tectal representation of the position of the optic nerve head. Thus, although the asymmetrical retinal histogenesis stabilizes the visual field position with respect to the body from stage 66 onwards, this selfsame asymmetry also forces small changes in the tectal projection of ganglion cells in the vicinity of the optic nerve head. This, of itself, will impose some requirement of visuomotor readjustment.

We turn, finally, to a problem thrown up by our data and implicit in the data of others. We do not know the answer to this problem but we present it for consideration. The problem relates to retinal histogenesis. We have presented evidence, in accord with others (Tay, Straznický & Hiscock, 1982; Straznický & Hiscock, 1984) that retinal histogenesis persists into the postmetamorphic period but at a progressively reducing rate, little histogenesis being evident later than 6 months after metamorphosis. From our retinal reconstructions we calculated that of the retina present one year after metamorphosis 29 % was produced after stage 64. Our cell density counts, in agreement with others (Graydon & Giorgi, 1984; Dunlop & Beazley, 1984) suggest little spatial heterogeneity in *Xenopus* retina. We might, therefore, expect the number of cells in the retinal ganglion cell layer to increase by 41 % ( $29/71 \times 100$ ) between stage 64 and one year after metamorphosis. In fact we find (Table 1) that such cells show an increase of 186 % in number during this period. Furthermore, between 1 year postmetamorphosis and adulthood a further 30 000 cells are added to this layer at a time when we are suggesting there is little histogenesis occurring.

These observations naturally raise the questions of where these cells are coming from and why their histogenesis has not been detected? The uniform cell densities across the retina, varying by no more than 50 %, suggest that the additional cells are not accumulating in the new retinal areas. They are appearing throughout the retina. It is, perhaps, possible that the additional cells are displaced from the inner nuclear layer. Alternatively, there may be sporadic cell division in the inner nuclear layer, some of the progeny of that division migrating to the retinal ganglion cell layer. This type of division was seen in late larval *Xenopus* by



Hollyfield (1971) and one instance of it can be seen in Fig. 7 of our data. Given the degree of the increase, however, one might have expected to see this much more frequently than we did.

This problem of undetected histogenesis in postmetamorphic *Xenopus* exists in an even greater form in the inner nuclear and outer nuclear retinal layers. We have not carried out systematic counts in these layers but examination of retinal sections reveals that the surface density of cells in the inner nuclear layer drops by about half between metamorphosis and adulthood while that of the receptor layer appears not to change. If this observation is correct, Beach & Jacobson (1979) also having noted no change in surface density of receptors in this period, it implies fairly massive histogenesis in these layers since surface area increases sixteen-fold in this period. Johns (1982) and Kock (1982) noted, in fish, that rod receptor density remained constant despite retinal expansion with age. Johns (1982) and Johns & Fernald (1981) provided evidence for interpolation of rods throughout the adult retina, these cells deriving from progenitors in the inner nuclear layer.

We are, therefore, suggesting that throughout the retina of postmetamorphic *Xenopus* additional cells are appearing in all retinal layers. It is disturbing that this histogenesis was not observed with our technique of single pulses of tritiated thymidine. It may be that the kinetics of cell division and of availability of tritiated thymidine are such that repeated administration of tritiated thymidine is required to detect the histogenesis.

We thank Mrs E. A. Dawes for preparation of the Figures and Mrs M. A. Hellon for typing the manuscript.

#### REFERENCES

- ABERCROMBIE, M. (1946). Estimation of nuclear population from microtome section. *Anat. Rec.* **94**, 239–247.
- BEACH, D. B. & JACOBSON, M. (1979). Patterns of cell proliferation in the retina of the clawed frog during development. *J. comp. Neurol.* **183**, 603–614.
- CHUNG, S.-H., BLISS, T. V. P. & KEATING, M. J. (1974). The synaptic organization of optic afferents in the amphibian tectum. *Proc. R. Soc. B* **187**, 421–447.
- CHUNG, S.-H., KEATING, M. J. & BLISS, T. V. P. (1974). Functional synaptic relations during the development of the retinotectal projection in amphibians. *Proc. R. Soc. B* **187**, 449–459.
- COOK, J. E., RANKIN, E. C. C. & STEVENS, H. P. (1983). A pattern of optic axons in the normal goldfish tectum consistent with caudal migration of optic terminals during development. *Expl Brain Res.* **52**, 147–151.
- DUNLOP, S. A. & BEAZLEY, L. D. (1984). A morphometric study of the retinal ganglion cell layer and optic nerve from metamorphosis in *Xenopus laevis*. *Vision Res.* **24**, 417–427.
- EASTER, S. S. & STUERMER, C. A. O. (1984). An evaluation of the hypothesis of shifting terminals in the goldfish optic tectum. *J. Neurosci.* **4**, 1052–1063.
- EDDS, M. V., JR, GAZE, R. M., SCHNEIDER, G. E. & IRWIN, L. N. (1979). Specificity and plasticity of retinotectal connections. *Neurosci. Res. Progr. Bull.* **17**, 243–375.
- FITE, K. V. (1973). The visual fields of the frog and toad; a comparative study. *Behav. Biol.* **9**, 707–718.
- FRASER, S. E. (1983). Fiber optic mapping of the *Xenopus* visual system: shift in the retinotectal projection during development. *Dev. Biol.* **95**, 505–511.

- GAZE, R. M. (1978). The problem of specificity in the formation of nerve connections. In *Specificity of Embryological Interactions. Receptors and Recognition*, vol. 4 (ed. D. R. Garrod), pp. 53–93. London: Chapman & Hall, Series B.
- GAZE, R. M., CHUNG, S.-H. & KEATING, M. J. (1972). Development of the retinotectal projection in *Xenopus*. *Nature (New Biology)* **236**, 133–135.
- GAZE, R. M., KEATING, M. J. & CHUNG, S.-H. (1974). The evolution of the retinotectal map during development in *Xenopus*. *Proc. R. Soc. B* **185**, 301–330.
- GAZE, R. M., KEATING, M. J., OSTBERG, A. & CHUNG, S.-H. (1979). The relationship between retinal and tectal growth in larval *Xenopus*: implications for the development of the retinotectal projection. *J. Embryol. exp. Morph.* **53**, 103–143.
- GIERER, A. (1983). Model for the retinotectal projection. *Proc. R. Soc. B* **218**, 77–93.
- GRANT, S. & KEATING, M. J. (1981). Changing patterns of neuronal connections during the normal maturation of the intertectal system in *Xenopus laevis*. *J. Physiol.* **320**, 18–19P.
- GRANT, S. & KEATING, M. J. (1985). Normal maturation involves systematic changes in binocular visual connections in *Xenopus laevis*. *Nature, Lond.* (in press).
- GRAYDON, M. L. & GIORGI, P. P. (1984). Topography of the retinal ganglion cell layer of *Xenopus*. *J. Anat.* **139**, 145–157.
- GROBSTEIN, P. & COMER, C. (1977). Post-metamorphic eye migration in *Xenopus* and *Rana*. *Nature, Lond.* **269**, 54–56.
- HOLLYFIELD, J. G. (1971). Differential growth of the neural retina in *Xenopus laevis* larvae. *Devl Biol.* **24**, 264–286.
- HOLT, C. E. & HARRIS, W. A. (1983). Order in the initial retinotectal map in *Xenopus*: a new technique for labelling growing nerve fibres. *Nature, Lond.* **301**, 150–152.
- JACOBSON, M. (1976). Histogenesis of the retina in the clawed frog with implications for the pattern of development of retinotectal connections. *Brain Res.* **103**, 541–545.
- JACOBSON, M. (1977). Mapping the developing retinotectal projection in frog tadpoles by a double-label autoradiographic technique. *Brain Res.* **127**, 55–67.
- JACOBSON, M. (1978). *Developmental Neurobiology*. 2nd Edition. New York: Plenum Press.
- JOHNS, P. R. (1982). Formation of photoreceptors in larval and adult goldfish. *J. Neurosci.* **2**, 178–198.
- JOHNS, P. R. & FERNALD, R. D. (1981). Genesis of rods in teleost fish retina. *Nature, Lond.* **293**, 141–142.
- KEATING, M. J. (1974). The role of visual function in the patterning of binocular visual connexions. *Brit. med. Bull.* **30**, 145–151.
- KOCK, J.-H. (1982). Neuronal addition and retinal expansion during growth of the crucian carp eye. *J. comp. Neurol.* **209**, 264–274.
- KONIGSMARK, B. W. (1970). Methods for the counting of neurons. In *Contemporary Research Methods in Neuroanatomy* (ed. W. J. Nauta & S. O. E. Ebbesson), pp. 315–339. Berlin: Springer-Verlag.
- LONGLEY, A. (1978). Anatomical mapping of retino-tectal connections in developing and metamorphosed *Xenopus*: evidence for changing connections. *J. Embryol. exp. Morph.* **45**, 249–270.
- MAROTTE, L. R. (1980). Goldfish retinotectal system: continuing development and synaptogenesis. *J. comp. Neurol.* **193**, 319–334.
- MEYER, R. L. (1978). Evidence from thymidine labelling for continuing growth of retina and tectum in juvenile goldfish. *Expl Neurol.* **59**, 99–111.
- MEYER, R. L. (1982). Ordering of retinotectal connections: a multivariate operational analysis. In *Current Topics in Developmental Biology* **17**, 101–145.
- NIEUWKOOP, P. D. & FABER, J. (1967). *Normal Table of Xenopus laevis (Daudin)*. Amsterdam: North-Holland.
- RAYMOND, P. A. & EASTER, S. S. (1983). Post-embryonic growth of the optic tectum in goldfish. I. Location of germinal cells and numbers of neurones produced. *J. Neurosci.* **3**, 1077–1091.
- REH, T. A. & CONSTANTINE-PATON, M. (1983). Qualitative and quantitative measures of plasticity during the normal development of the *Rana pipiens* retinotectal projection. *Devl Brain Res.* **10**, 187–200.
- REH, T. A. & CONSTANTINE-PATON, M. (1984). Retinal ganglion cell terminals change their projection sites during larval development of *Rana pipiens*. *J. Neurosci.* **4**, 442–457.

- SCOTT, T. M. (1974). The development of the retinotectal projection in *Xenopus laevis*: an autoradiographic and degeneration study. *J. Embryol. exp. Morph.* **31**, 409–414.
- SCOTT, T. M. & LAZAR, G. (1976). An investigation into the hypothesis of shifting neuronal relationship during development. *J. Anat.* **121**, 485–496.
- SPERRY, R. W. (1943). Visuomotor coordination in the newt (*Triturus viridesens*) after regeneration of the optic nerve. *J. comp. Neurol.* **79**, 33–55.
- SPERRY, R. W. (1944). Optic nerve regeneration with return of vision in anurans. *J. Neurophysiol.* **7**, 57–69.
- SPERRY, R. W. (1951). Mechanisms of neural maturation. In *Handbook of Experimental Psychology* (ed. S. S. Stevens), pp. 236–280. New York: J. Wiley & Sons.
- STEVENSON, J. A. & YOON, M. G. (1981). Mitosis of radial glial cells in the optic tectum of adult goldfish. *J. Neurosci.* **1**, 862–875.
- STRAZNICKY, C. & GAZE, R. M. (1971). The growth of the retina in *Xenopus laevis*: an autoradiographic study. *J. Embryol. exp. Morph.* **26**, 67–79.
- STRAZNICKY, C. & GAZE, R. M. (1972). The development of the tectum in *Xenopus laevis*: an autoradiographic study. *J. Embryol. exp. Morph.* **28**, 87–115.
- STRAZNICKY, C. & HISCOCK, J. (1984). Post-metamorphic retinal growth in *Xenopus*. *Anat. Embryol.* **169**, 103–109.
- TAY, D., HISCOCK, J. & STRAZNICKY, C. (1982). Temporo-nasal asymmetry in the accretion of retinal ganglion cells in late larval and post-metamorphic *Xenopus*. *Anat. Embryol.* **164**, 75–83.
- UDIN, S. B. & KEATING, M. J. (1981). Plasticity in a central nervous pathway in *Xenopus*: anatomical changes in the isthmotectal projection after larval eye rotation. *J. comp. Neurol.* **203**, 575–594.

(Accepted 9 September 1985)